Research Report

2004-01

Analysis and Control of Three Phase AC/DC PWM Converter Under Unbalanced Operating Conditions.

B.A. Welchko, T.M. Jahns*, T.A. Lipo*

General Motors Advanced Technology Center
3050 Lomita Blvd.
Torrance, Ca 90905, USA
bwelchko@ieee.org

*Dept. of Electrical and Computer Engineering
University of Wisconsin-Madison
1415 Engineering Dr.
Madison, WI, 53706, USA
jahns@engr.wisc.edu, lipo@engr.wisc.edu

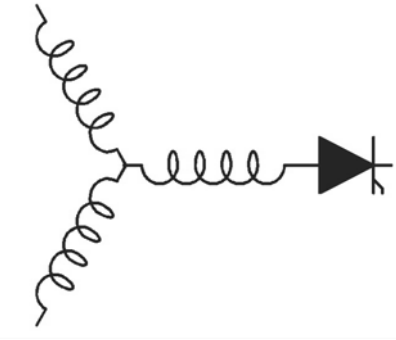

Wisconsin
Electric
Machines &
Power
Electronics
Consortium

University of Wisconsin-Madison
College of Engineering
Wisconsin Power Electronics Research Center
2559D Engineering Hall
1415 Engineering Drive
Madison WI 53706-1691

Short-Circuit Fault Mitigation Methods for Interior PM Synchronous Machine Drives using Six-Leg Inverters

Brian A. Welchko
General Motors Advanced Technology Center
3050 Lomita Blvd.
Torrance, CA 90905, USA
bwelchko@ieee.org

Thomas M. Jahns*
Thomas A. Lipo*
*Department of Electrical and Computer Engineering
University of Wisconsin-Madison
1415 Engineering Dr.
Madison, WI 53706, USA
jahns@engr.wisc.edu; lipo@engr.wisc.edu

Abstract – **This paper characterizes six-leg inverters to mitigate short-circuit faults for interior permanent magnet (IPM) synchronous machines. Key differences between bus structures in six-leg inverters are identified. For six-leg inverters employing two isolated dc links, it is shown that up to 75% of rated output power could be produced following a single-switch short-circuit fault. A magnet flux nulling control method is proposed as a response to stator winding type short-circuit faults. This control method results in a zero-torque fault response by the motor. The important influence of the zero sequence in both the motor and inverter structure is identified and developed for this class of fault. Simulation and experimental results are presented verifying the proposed magnet flux nulling control method.**

I. INTRODUCTION

INTERIOR PERMANENT MAGNET (IPM) synchronous machines are attractive for a variety of applications because of their high power density, wide constant power speed range, and excellent efficiency [1], [2]. However, the adoption of permanent magnet synchronous machines in applications such as electric propulsion has been hindered by concerns about the special risks posed by faults in these machines. During normal operation, the magnets provide an inherent flux in the machine so that a larger percentage of the applied current can be used to produce torque. In the presence of any type of system fault, either originating in the machine or the electronic drive, the magnets become an immediate liability since their location in the spinning rotor produces a source of flux which cannot be turned off at will.

The area of fault analysis and fault mitigation is quite broad due to the seemingly infinite number of possibilities which can occur. Essentially, any undesired event outside of normal operation can be considered a fault. One serious fault which is likely to occur due to a software error is an Uncontrolled Generator Mode (UCG) fault [3], [4]. For this fault, the gating signals are removed from the inverter switches and the machine may regenerate energy back to the dc link. Various faults originating due to failures in different parts of the electronic drive have been investigated, of which, [5] provides a good example for PM machine drives. A more detailed study of open-circuit type faults was investigated in [6], while a similar detailed analysis was carried out for short-circuit type faults in [7].

In [7], it was shown that the preferred post-fault control strategy for a single-switch short-circuit fault was to employ the remaining healthy drive switches to command a symmetrical three-phase short-circuit on the terminals of the IPM motor. This had the effect of reducing the post-fault currents and motor breaking torque. For open-circuit type faults, [6] showed that commanding UCG response resulted in the lowest obtainable currents and (braking) torque. Both of these strategies are reactionary in nature. That is, the system detects a fault and performs an action (close or open switches) and then waits for further instruction, which is presumably, a system shutdown.

This paper presents an active response to system-level faults so that the system can continue to operate with some reduced capacity. The paper specifically shows that by employing a cascaded inverter topology, up to 75% of the rated system power can be achieved following a single-switch short-circuit fault. Topological similarities between a single inverter switch short-circuit fault and a motor winding short-circuit fault are also identified. These similarities are used to develop a control method to null the magnet flux by active control of the remaining healthy motor phases in order to produce a zero-torque response by the motor in a post-fault condition.

II. DRIVE SYSTEM TOPOLOGY

The use of single-phase inverters for each phase of an ac machine is relatively common if the machine is of the switched reluctance type, due to the rectangular phase currents which must be employed. For PM motors, the use of multiple single-phase inverters provides a higher degree of flexibility and redundancy when compared to a standard six-switch, three-phase inverter. Many different possible implementations of this class of topology are possible, each with subtle differences. Therefore, consider a general six-leg inverter driving a three-phase ac motor. Note that in all cases, it is a requirement that both ends of each stator phase winding are available.

The most general format of the six-leg inverter topology is shown in Fig. 1. In this configuration, each phase of the motor is excited by a single-phase inverter. Using this building block approach, three isolated dc supplies are required.

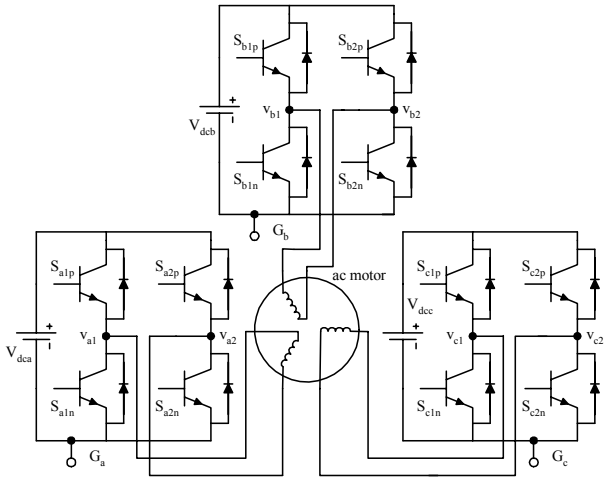

Fig. 1. Three single-phase inverters driving a three-phase ac motor.

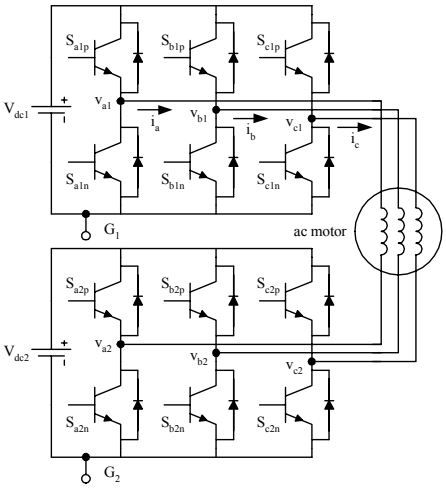

Fig. 2. Cascaded converter with separate dc links.

It is possible to simplify the topology of Fig. 1 by repartitioning the phase-legs into three-phase groups. The result has previously been referred to as a cascaded converter and is shown in Fig. 2. It is possible to obtain this implementation of the topology simply by using two standard three-phase inverters and changing the control method. This configuration with isolated dc links is sometimes used as an alternative implementation of a three-level inverter [8], [9].

In some instances, isolation between the dc links of the cascaded converter is either not available, or undesirable. As a result, the cascaded converter system of Fig. 3 is obtained. Due to the presence of only a single dc link, the configuration of Fig. 3 could be repartitioned into a true six-leg inverter system as shown in Fig. 4.

The inverter configurations in Fig. 1, Fig. 3, and Fig. 4 are functionally equivalent while the configuration of Fig. 2 is unique. The critical difference is in the isolation between the two dc links in Fig. 2. In this case, the system can apply a true square wave voltage excitation across each phase of the motor. A square wave excitation produces triplen harmonic voltages. In all of six-leg inverter circuits, the zero sequence return path is through the dc links. If the two links are isolated, the circuit is not complete and the triplen

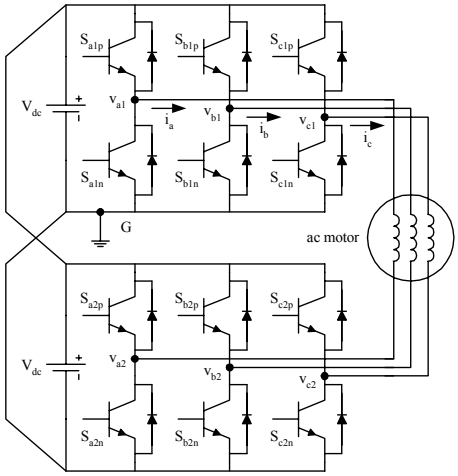

Fig. 3. Cascaded converter with connected dc links.

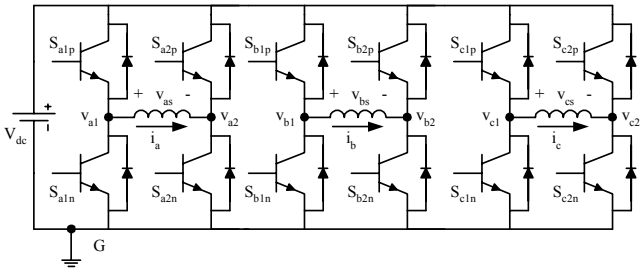

Fig. 4. Six-leg converter with a single dc bus.

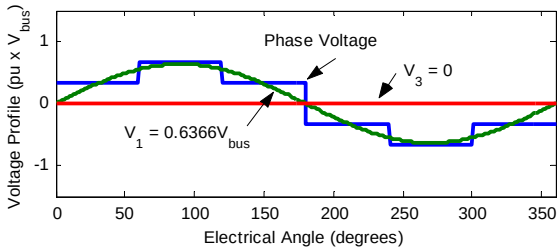

(a) Standard three-leg inverter voltage components in six-step operation.

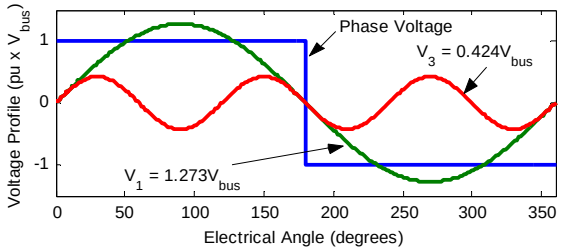

(b) Six-leg inverter voltage components in square wave operation.

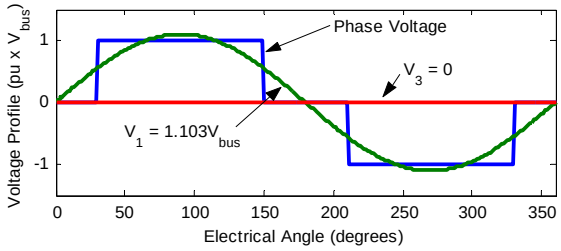

(c) Maximum six-leg inverter voltage components without a third harmonic.

Fig. 5. Inverter voltage profiles showing applied voltage, fundamental, and third harmonic components.

and zero sequence voltages do not induce any currents. If there are one or three dc links, the zero sequence voltage must be precisely controlled so that zero sequence currents are minimized or eliminated. This also has the effect of reducing the maximum fundamental output voltage component which can be generated [10]. Fig. 5 shows the overmodulation voltage limits for six-leg inverters along with the familiar six-step limits for standard three-leg inverters as a reference.

III. Inverter Output Capacity

The voltage space of the six-leg inverter system can be represented in space vector format as shown in Fig. 6 ($V_{dc1} = V_{dc2}$). The figure shows that the system has the identical space vector diagram as a three-level neutral point clamped (NPC) converter. Employing nomenclature used for the NPC inverter, a level-2 output indicates the largest positive voltage connected across the phase load, a level-0 output indicates the largest negative voltage across the phase load, and a level-1 output indicates that zero volts is being applied across the phase. Not shown in the figure are the high numbers of redundant states in the cascaded system. In this space vector diagram, there are 19 distinct inverter states. For the six-leg topology, there are $4^3 = 64$ output states, compared with $3^3 = 27$ outputs for a traditional NPC inverter. The increased number of states is a result of two possible level-1 output states in each leg.

In the presence of a short-circuit type fault applied to the lower switch in phase *a* (switch S_{a1n}), the six-leg inverter is capable of outputting a level-1 output on the faulted phase by closing the adjacent switch in the faulted H-bridge. It is also possible for the faulted phase to command a level-0 output. The resulting voltage space in space vector format of the cascaded converter system, with a single-switch short-circuit fault, is also shown in Fig. 6 as the shaded area. Following the single-switch short-circuit fault, it is still possible to control both the *d*- and *q*-axis voltages simultaneously, since a circle centered at the origin can be inscribed in the distorted hexagon. This circle is half as large as during normal operation. It is further possible to increase the size of the circle, which can be inscribed inside the faulted hexagon, to 75% of the original size, by employing a shift in the neutral voltage, as shown in Fig. 6. Shifting the neutral point of the motor, in the case of the open winding machine, is strictly a mathematical representation, since there is no physical neutral point from which to measure a voltage. As a result, it is a useful control technique to extend the operating range of the system with a single-switch short-circuit fault. The interested reader is referred to [11] for additional background information on the general case for multi-level systems.

However, as with any promising technique, the potential drawbacks must be considered. In this case, the technique is only applicable to the dual bus system of Fig. 2 due to the presence of a zero sequence component which would induce large currents in systems containing three or one dc links.

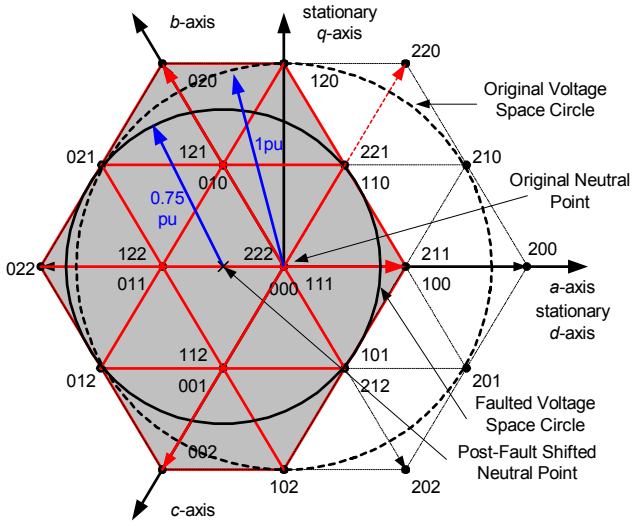

Fig. 6. Voltage space limits for pre- and post-fault single-switch short-circuit conditions for the six-leg inverter.

IV. Magnet Flux Nulling Control

One of the more severe faults that can occur in any motor drive system is a shorted or partially shorted coil in one of the motor's stator windings. This fault requires immediate attention to prevent the motor from overheating. This type of fault has been investigated in terms of operation with a shorted coil for synchronous reluctance machines [12].

A. Current Control Method

For considerations of modeling, it will be assumed that the phase *a* coil is fully shorted. This serves two purposes. In the case of a partially shorted winding coil, the coil can be made to appear fully shorted via active control of the faulted phase by simply closing two of the switches in the six-leg inverter. In the case of a single-switch short-circuit fault, the control action could also close the complimentary switch, which would also make the system appear as if one of the stator windings was shorted out.

In the presence of a shorted or partially shorted stator winding, it is desirable to make the current in the faulted phase as small as possible. Therefore, it is required to make the flux linkage in the shorted coil as constant as possible. From the machine model of an IPM motor, the flux linkages are given as

$$\lambda_d^e = L_d i_d^e + \Psi_{mag} \tag{1}$$

$$\lambda_q^e = L_q i_q^e \tag{2}$$

$$\lambda_0^e = L_0 i_0^e . \tag{3}$$

Since the fault occurs in the stationary frame, it is required to transform the synchronous fluxes back to the stationary reference frame. Applying the transformation gives

$$\lambda_d^s = -\left(\sin\theta_e\right) L_q i_q^e + \left(\cos\theta_e\right)\left(L_d i_d^e + \Psi_{mag}\right) \tag{4}$$

$$\lambda_q^s = \left(\cos\theta_e\right) L_q\, i_q^e + \left(\sin\theta_e\right)\left(L_d\, i_d^e + \Psi_{mag}\right) \quad (5)$$

$$\lambda_0^s = L_0\, i_0^e . \quad (6)$$

It will be assumed that the fault occurs in phase *a*. From the reference frame definitions and (4) – (6), the phase *a* flux linkage is given as

$$\lambda_a = -\left(\sin\theta_e\right) L_q\, i_q^e + \left(\cos\theta_e\right)\left(L_d\, i_d^e + \Psi_{mag}\right) + L_0\, i_0^e . \quad (7)$$

The simplest case of a constant flux linkage in phase *a* occurs when the flux in the phase is zero. Using this, (7) can be rearranged as

$$\Psi_{mag}\cos\theta_e = L_q\, i_q^e \sin\theta_e - L_d\, i_d^e \cos\theta_e - L_0\, i_0^e . \quad (8)$$

Equation (8) indicates the conditions required to yield a phase *a* flux linkage of zero. Since the zero sequence inductance of the motor is typically quite small when compared to either the *q*- or *d*-axis inductance, it can momentarily be neglected for the proceeding control method. As a result, (8) simplifies to

$$\Psi_{mag}\cos\theta_e = L_q\, i_q^e \sin\theta_e - L_d\, i_d^e \cos\theta_e . \quad (9)$$

Setting the *q*-axis current to zero and solving (9) for the *d*-axis current yields

$$i_d^e = -\frac{\Psi_{mag}}{L_d} . \quad (10)$$

Equation (10) indicates that setting the *d*-axis current to the motor's characteristic current will null the magnet flux. Without a *q*-axis current, the net torque of the motor will be zero. This result is a significant improvement over the previously proposed method of creating a symmetrical three-phase short-circuit as a response to short-circuit type faults, as the symmetrical three-phase short-circuit produced a potentially significant amount of braking torque [7], while this proposed method produces zero torque.

B. Voltage Control Limitations

While current is the quantity which is typically controlled in any vector controlled motor drive, it is only indirectly controlled, as voltage from the switch states is ultimately the manipulated variable. Fig. 7 shows the block diagram for a standard synchronous frame current regulator for an IPM synchronous machine [13]. Included in the current regulator, are cross-coupling decoupling terms and a back-emf decoupling term. In addition, the zero sequence current regulator is shown, since that must be a controlled quantity in the six-leg inverter without two dc links.

Consider the phase *a* voltage command which results from the current regulator. After transformation back to the stationary reference frame, it is given as

$$v_a^{s*} = v_d^{s*} + v_0^{s*} . \quad (11)$$

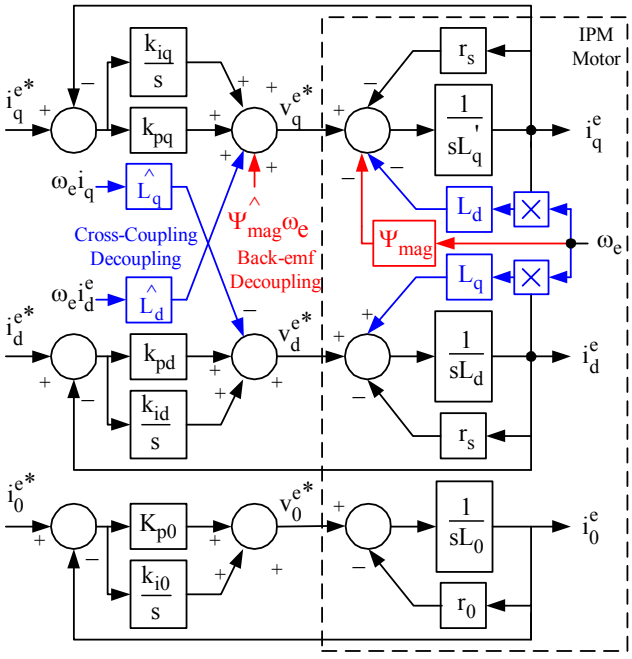

Fig. 7. Block diagram of the cross-coupling decoupling synchronous frame current regulator for IPM motor drives.

Under the proposed control method for the shorted coil fault, v_d^{s*} will be some time varying quantity while v_0^{s*} will be zero. Due to the constraint of the short-circuit, it is required that $v_a^{s*} \equiv 0$ at every instance. As a result, (11) indicates that it is not possible to independently control the *q*-, *d*-, and 0-axis voltages simultaneously during the faulted condition. In an unfaulted system, it is possible to independently control the *q*-, *d*-, and zero sequence voltages within a sphere centered at the origin [14]. If the *d*-axis voltage is the controlled quantity and the phase is shorted due to the fault, (11) indicates that the applied zero sequence voltage will be

$$v_0^{s*} = -v_d^{s*} . \quad (12)$$

In six-leg inverter systems which employ one or three isolated dc links, a zero sequence current path is present. Employing the constraint of (12), the steady-state zero sequence current induced in the shorted phase is

$$i_{0\_ss} = \frac{\left|v_d^{e*}\right|}{\sqrt{r_s^2 + \left(\omega L_0\right)^2}} \angle\left(180° - \operatorname{atan}\left(\frac{\omega L_0}{r_s}\right)\right) . \quad (13)$$

Equation (13) indicates that for small values of L_0 (ideally zero) and low frequencies, the induced zero sequence current will ideally be the negative of the stationary frame *d*-axis current needed to null the magnet flux, torque, and induced current in the shorted phase. For non-ideal values of L_0, some current will be induced in the shorted phase.

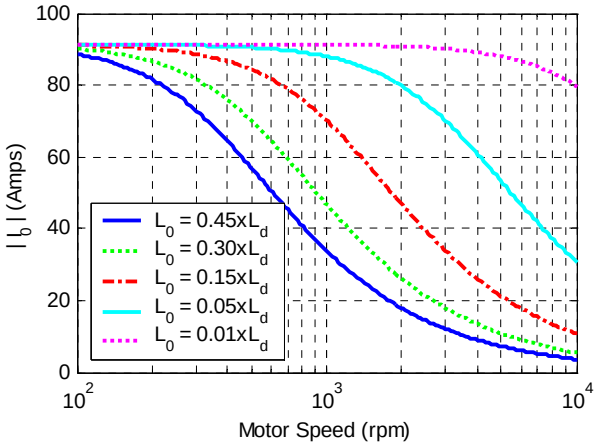

Fig. 8. Induced zero sequence current with magnet flux nulling control.

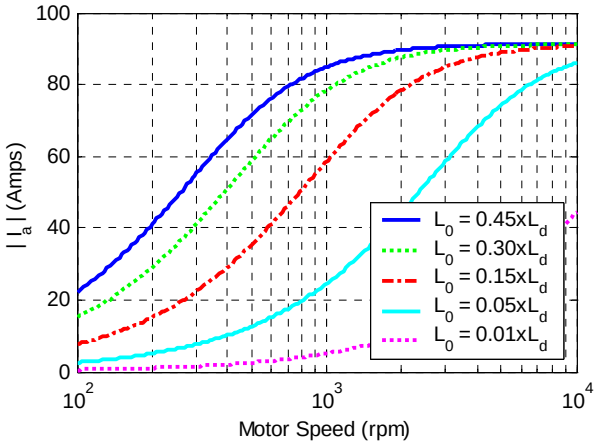

Fig. 9. Induced current in the shorted phase when employing magnet flux nulling control following a shorted stator winding.

Fig. 8 and Fig. 9 show the steady-state amplitudes of the zero sequence current and current induced in the shorted phase as a function of speed for various values of zero sequence inductance for the IPM motor of reference [15] (see appendix). In general, the figures and analysis show that the zero sequence current induced at low speed is approximately the characteristic current (93.3 A_{peak} for this example) and asymptotes toward zero at high speed. For the current in the shorted phase, the opposite is true; the current at low speed is low and asymptotes to the characteristic current at high speed. It is important to note that even though the zero sequence current is induced and uncontrolled, the torque will still be zero due to the synchronous frame control on the *d*- and *q*-axis currents.

V. Simulation and Experimental Results

The proposed control algorithm to null the magnet flux following a short-circuit fault in phase *a* was simulated in Simulink® with data post-processing in MATLAB®. Both the simulation and experimental results employed the IPM motor (of the appendix) and the *dq0* synchronous frame current regulator of Fig. 7 tuned to a bandwidth of 700 Hz. The *d*-axis inductance used for the simulation was obtained by measuring the open-circuit magnet flux based back-emf and symmetrical three-phase short-circuit current at high

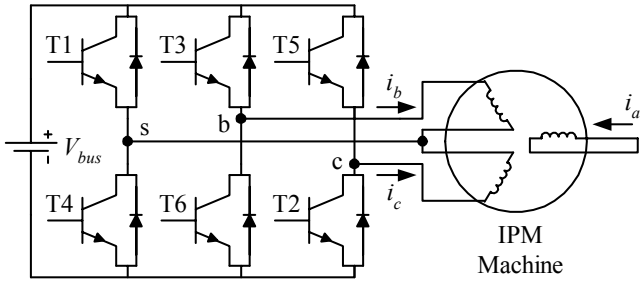

Fig. 10. Experimental drive configuration.

speed. From these measured values, the *d*-axis inductance is given as 91.5 μH. The zero sequence inductance was found to be 45% of this value, or 41.2 μH.

As proposed, the flux nulling control method employs a six-leg inverter. The available experimental dynamometer setup employed a standard three-phase, three-leg inverter. As a result, it was necessary to reconfigure the system, as shown in Fig. 10, in order to test the proposed flux nulling control method. Phase *a* of the motor was externally shorted together as shown to emulate a level-1 output by phase *a* of the desired six-leg inverter. The center point, *s*, of phases *b* and *c*, was tied together and connected to the traditional phase *a* output of the inverter to allow for independent control of the currents in phases *b* and *c*. For the tests, all three of the phase currents were measured, and used by the controller as needed. The motor speed was controlled externally by the dynamometer.

Simulation and measured experimental results for both low-speed (150 rpm) and high-speed (1000 rpm) operation are shown overlaid on one another in Fig. 11 and Fig. 12. It should be noted that the experimental torque results presented were not directly measured, but calculated using the measured currents and estimated motor parameters.

In both cases, the measured value of the phase currents, and hence the synchronous frame *dq0* currents, match very closely in both shape and amplitude to the simulation results. The phase *a* current which is induced due to the zero sequence inductance, contains evidence of a third harmonic component which is likely due to the slotting effect of the stator winding and magnet cavities, and has been neglected in the simulations.

The value of the zero sequence current decreases as the speed increased as predicted in Section IV. Also as predicted, the current in the shorted phase increases as the speed increases. Both of these are due to the coupling effect of the zero-sequence inductance. From this result are two very important implications which must be considered. First, it has the effect of unbalancing the two remaining active healthy phases. While the unbalance is not really important, the relative amplitudes of the currents in these two phases are; because they are both larger than the characteristic current of the motor given by Ψ_{mag}/L_d (93.3 A_{peak}). If the zero sequence inductance was the ideal value of zero, these currents would be larger than the characteristic current by a multiple of $\sqrt{3}$, which represents an upper limit for the value of the current in the healthy phases. This observation implies that in order to have the

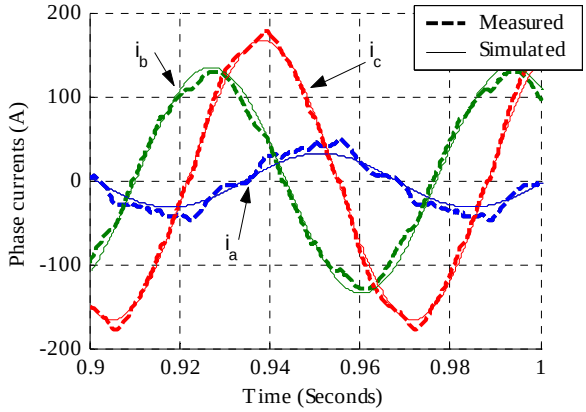

(a) Phase currents.

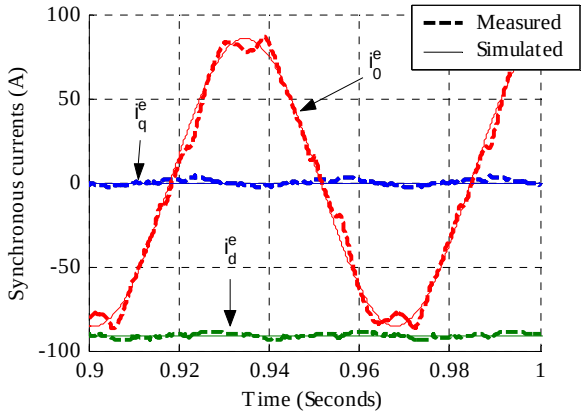

(b) Synchronous frame *dq0* currents.

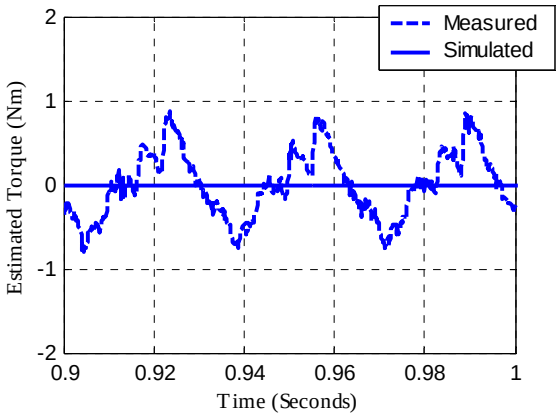

(c) Estimated motor torque.

Fig. 11. Experimental and simulated results at 150 rpm.

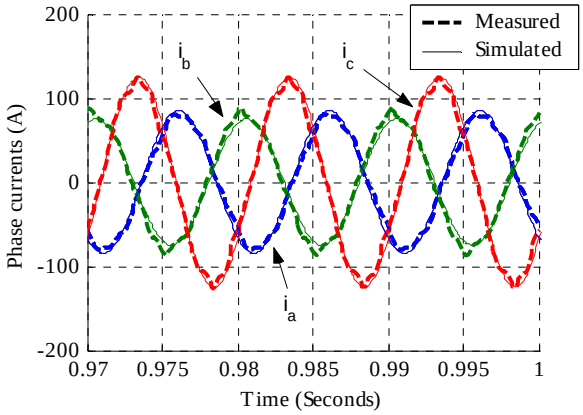

(a) Phase currents.

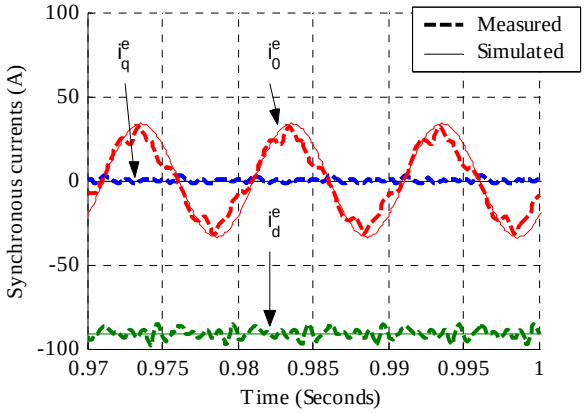

(b) Synchronous frame *dq0* currents.

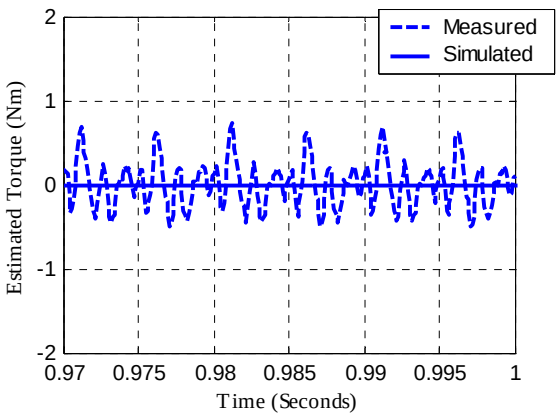

(c) Estimated motor torque.

Fig. 12. Experimental and simulated results at 1000 rpm.

option of employing the proposed flux nulling control method, the system has to be designed such that the motor's characteristic current is less than $1/\sqrt{3}$ times the value of the rated current of the inverter so that the inverter current limit is not exceeded. The second important observation is that when synchronous frame *dq0* current control is employed, the current in the shorted phase will asymptote out to the value of the characteristic current at high speeds.

In terms of torque production, the measured estimated torque is pulsating in nature, but always less than 1 Nm in amplitude, while the simulated torque is always zero due the synchronous frame current control and an ideal motor model. The average measured torque obtained by a torque meter was found to be +0.59 Nm and –0.27 Nm for the 150 rpm and 1000 rpm cases respectively. This compares to a measured torque of –4.69 Nm and –1.63 Nm which was obtained when

a symmetrical three-phase short-circuit was employed as a response to a short-circuit condition as was proposed in [7]. As a result, the proposed flux nulling control technique produces a near zero-torque response in response to a short-circuit fault or shorted winding type fault which is an improvement over previously proposed solutions.

VI. Conclusions

This paper has investigated the modeling and control of fault mitigation strategies for interior permanent magnet synchronous machines driven by a six-leg inverter. As possible implementations of the six-leg inverter, four configurations were considered with the difference being in the number and isolation of the dc links in the system. Faults considered were switch-short circuit faults and full or partial stator winding short-circuit faults.

It was shown that if a cascaded converter is employed with isolation between the two dc links, the system is able to output the full rated system current at up to 3/4 the rated system voltage in the presence of a single-switch short-circuit fault. Due to zero sequence voltage limitations, this benefit is not possible with other implementations of a six-leg inverter.

A flux nulling control method was proposed as a method to produce a zero-torque response by the motor following a single-switch short-circuit fault, or a full or partial stator winding short-circuit fault. The influence of the zero sequence inductance on the induced current in the faulted phase was characterized for systems which contain a zero sequence conduction path. At low speeds, the healthy phase currents are limited to $\sqrt{3}\,\Psi_{mag}/L_d$ or less while at high speeds the current in the faulted phase asymptotes to Ψ_{mag}/L_d. Both simulation and experimental results confirmed the proposed flux nulling *dq0* synchronous frame current control method.

As a final note, this paper has reinforced the notion that the machine design and control must be carefully coordinated. This is necessary to insure desirable fault response properties so that the system meets fault tolerance requirements while maintaining the desirable qualities of IPM machines during normal operation.

Appendix
Interior PM Machine Parameters

3 phase, 6 kW peak at 6000 rpm, 12 pole machine with

$r_s \approx 0.0103\ \Omega$ $\quad \Psi_{mag} \approx 5.91\ \mathrm{mW_{rms}}$ $\quad L_d \approx 91.5\ \mu\mathrm{H}$
$L_{qmax} \approx 305\ \mu\mathrm{H}$ $\quad C_1 \approx 0.0058\ \mathrm{H/Amp}$ $\quad C_2 \approx -0.605$

where the *q*-axis inductance is approximated as

$$L_q \approx L_{qmax} \text{ or } C_1 \left| i_q^e \right|^{C_2}$$

whichever is smaller.

Acknowledgments

The authors would like to acknowledge the support and motivation provided by the member companies of the Wisconsin Electric Machines and Power Electronics Consortium (WEMPEC) at the University of Wisconsin-Madison. The authors thank Dr. Hyunbae Kim and Mr. Jackson Wai of the University of Wisconsin-Madison for their assistance in collecting the experimental results.

References

[1] W. L. Soong, *"Design and modeling of axially-laminated interior permanent magnet motor drives for field-weakening applications,"* Ph.D. Dissertation, Dept. of Electronics and Elec. Eng., Univ. of Glasgow, Glasgow, U.K., Sept. 1993.

[2] T. M. Jahns, G. B. Kliman, and T. W. Neuman, "Interior PM synchronous motors for adjustable speed drives," *IEEE Trans. Ind. Applicat.*, vol. IA-22, no. 4, pp. 738-747, July/August 1986.

[3] T. M. Jahns, and V. Caliskan, "Uncontrolled generator operation of interior PM synchronous machines following high speed inverter shutdown," *IEEE Trans. Ind. Applicat.*, vol. IA-35, no. 6, pp. 1347-1357, Nov/Dec 1999.

[4] A. Adnanes, R. Nilssen, and R. Rad, "Power feed-back during controller failure in inverter fed permanent magnet synchronous motor drives with flux weakening," in *Conf. Rec. IEEE PESC*, 1992, vol. 2, pp. 958–963.

[5] N. Bianchi, S. Bolognani, and M. Zigliotto, "Analysis of PM synchronous motor drive failures during flux weakening operation," in *Conf. Rec. IEEE PESC*, 1996, vol. 2, pp. 1542-1548.

[6] B. A. Welchko, T. M. Jahns, and S. Hiti, "IPM synchronous machine drive response to a single-phase open circuit fault," *IEEE Trans. Power Electron.*, vol. 17, no. 5, pp. 764-771, Sept. 2002.

[7] B. A. Welchko, T. M. Jahns, W. L. Soong, and J. M. Nagashima, IPM synchronous machine drive response to symmetrical and asymmetrical short circuit faults," *IEEE Trans. Energy Conversion*, vol. 18, no. 2, pp. 291-298, June 2003.

[8] H. Stemmler and P. Guggenbach, "Configurations of high-power voltage source inverter drives," in *5th European Conference on Power Electronics and Applications (EPE)*, 1993, vol. 5, pp. 7-14.

[9] K. A. Korzine, S. D. Sudhoff, and C. A. Whitcomb, "Performance characteristics of a cascaded two-level converter," *IEEE Trans. Energy Conversion*, vol. 14, no. 3, pp. 433-439, 1999.

[10] B. A. Welchko, *"Contributions to the reduced cost and increased reliability of permanent magnet synchronous machine drives,"* Ph.D. Dissertation, Dept. of Electrical and Computer Engineering, Univ. of Wisconsin, Madison, WI, 2003.

[11] P. W. Hammond, "Enhancing the reliability of modular medium-voltage drives," *IEEE Trans. on Industrial Electronics*, vol. 49, no. 5, pp. 948-954, Oct. 2002.

[12] D. Qin, X. Lua, and T. A. Lipo, "Reluctance motor control for fault-tolerant capability," in *Conf. Rec. IEEE IEMDC*, 1997, pp. WA1-1.1-WA1-1.6.

[13] H. Kim, and R. D. Lorenz, "Improved current regulators for IPM machine drives using on-line parameter estimation," in *Conf. Rec. IEEE IAS Annual Meeting*, 2002. vol. 1, pp. 86-91.

[14] M. J. Ryan, R. W. De Doncker, and R. D. Lorenz, "Decoupled control of a four-leg inverter via a new 4×4 transformation matrix," *IEEE Trans. Power Electronics*, vol. 16, no. 5, pp. 694-701, Sept. 2001.

[15] E. C. Lovelace, T. M. Jahns, J. Wai, T. Keim, J. H. Lang, D. D. Wentzloff, F. Leonardi, J. M. Miller, and P. J. McCleer, "Design and experimental verification of a direct-drive interior PM synchronous machine using a saturable lumped-parameter model," in *Conf. Rec. IEEE IAS Annual Meeting*, 2002, vol. 4, pp. 2486-2492.